

Development of Comprehensive Two-Dimensional High Temperature Liquid Chromatography \times Gel Permeation Chromatography for Characterization of Polyolefins.

Abhishek Roy,[†] Matthew D. Miller,^{*,‡} David M. Meunier,^{*,||} A. Willem deGroot,[‡] William L. Winniford,[‡] Freddy A. Van Damme,[§] Randy J. Pell,^{||} and John W. Lyons^{*,||}

[†]Filmtec Corporation, Filmtec R&D, Edina, MN 55439, [‡]The Dow Chemical Company, Freeport, TX 77541,

[§]Dow Benelux, Terneuzen 4530 AA, The Netherlands, and ^{||}The Dow Chemical Company, Midland, Michigan 48667

Received January 4, 2010; Revised Manuscript Received March 17, 2010

ABSTRACT: This work documents the development of the title system wherein the first dimension is a separation of polyolefins, according to composition, via an adsorption mechanism on a HYPERCARB stationary phase, and the second dimension is a separation of polyolefins on a gel permeation chromatography (GPC) column. Proper optimization of the experimental parameters including high temperature liquid chromatography (HTLC) flow rate, GPC flow rate, GPC column type, and solvent gradient program enabled successful operation of the two-dimensional (2D) system. Two angle light scattering at 90° and 15° and solution infrared absorbance detectors were used for qualitative and quantitative analysis of the 2D data. Apparent composition distribution, apparent molecular weight distribution, and the complete two-dimensional (composition \times molecular weight) distribution were obtained for a given polymer. This system is an improvement over a prior two-dimensional system based on temperature rising elution fractionation (TREF)/GPC in that TREF has difficulty separating polyolefins by composition if the polyolefins contain more than approximately 8 mol percent comonomer. Polyolefins synthesized from different catalysts (Metallocene and Ziegler–Natta) showed differences in the molecular weight, composition and number of resolved species in their respective 2D HTLC–GPC chromatograms as a function of catalyst type. Although the polymers studied here were all polyolefins, this approach can also be extended to other polymers.

Introduction

Developments in catalysis combined with advances in process technology allow improved control of the molecular architecture of polyolefins for designing resins for targeted applications. In order to take full advantage of this new control, it is essential that the structure/property relationships are well established for a given application. Establishing these relationships requires a modern tool box of polymer molecular structure characterization techniques. For the past few years, significant research has been conducted at The Dow Chemical Company as well as in other laboratories to develop high temperature gradient liquid chromatography (HT–LC) techniques for fractionating polyolefins according to composition. In the first example of gradient liquid chromatography applied to olefin-based copolymers, poly(ethylene-*co*-styrene) materials were fractionated by chemical composition at a temperature between 30 and 80 °C.¹ A two-dimensional, temperature rising elution fractionation (TREF)/gel permeation chromatography (GPC) system for cross-fractionation of olefin copolymers was developed.² Crystallization elution fractionation (CEF) has been developed to quickly characterize the composition distributions of polyolefin materials that exhibit at least some degree of crystallinity.^{3,4} TREF⁵ and crystallization analysis fractionation (CRYSTAF)^{6,7} separation schemes have been used for many years to characterize composition distributions of semicrystalline polymers.

In this work, the composition characterization dimension does not depend on crystallinity at all. Indeed, the first dimension

separation is carried out at temperatures above the crystalline melting temperatures, T_M , of polyolefins, thus rendering them noncrystalline. Thus, this work enables the generation of two-dimensional characterization data, like the TREF/GPC system does, but over a wider composition range than is possible when using TREF as the first dimension.

Recently a partnership between The Dow Chemical Company and Deutsches Kunststoff-Institut (DKI) demonstrated the separation of randomly polymerized poly(ethylene-*co*-octene) (EO) copolymers at 140 °C using a gradient solvent of 1,2,4-trichlorobenzene (TCB) and ethylene glycol monobutyl ether as the mobile phase.⁸ The stationary phase used was silica, and the mechanism of separation is believed to be precipitation and redissolution driven by the solubility of the copolymer. The resolution of the precipitation/redissolution scheme was low, consistent with prior observations for a precipitation/redissolution scheme.¹

The use of a graphite stationary phase (Hypercarb), which resulted in a much better separation of randomly polymerized EO and poly(ethylene-*co*-propylene) (EP) copolymers as a function of composition, was recently discovered.⁹ Researchers at DKI have also investigated the separation of polyolefins according to composition.^{10,11}

In contrast to a precipitation/redissolution mechanism, the graphite stationary phase is believed to provide retention primarily based on an adsorption mechanism, and much higher resolution separations are easily achieved. The technique readily allows one to estimate the chemical composition distribution in a short period of time. Structural features of polyolefins that affect such separations include composition, size of the short-chain branches, tacticity, microstructure, and molecular weight for

*To whom correspondence should be addressed. E-mail: (M.D.D.) Dmiller4@Dow.com; (D.M.M.) DMeunier@Dow.com; (J.W.L.) JWLyons@Dow.com.

Table 1. Summary of the Materials Studied

Figure	sample	chemical composition
1	poly(ethylene- <i>co</i> -octene) copolymer	14.8 mol % octene
2	poly(ethylene- <i>co</i> -octene) copolymer	15.9 mol % octene
3	poly(ethylene- <i>co</i> -octene) copolymer	15.9 mol % octene
4	poly(ethylene- <i>co</i> -octene) copolymers	0, 2.6, 8.5, 14.8, 15.9, 19.6, 24.3, and 100 mol % octene
5	poly(ethylene- <i>co</i> -octene) copolymers	0, 2.6, 8.5, 14.8, 15.9, 19.6, 21.7, 24.3, and 56 mol % octene
7	poly(ethylene- <i>co</i> -octene) copolymers	2.6, 8.5, 14.8, 19.6 mol % octene
8	metallocene catalyzed homopolyethylenes	
9	50–50 wt % blend of poly(ethylene- <i>co</i> -octene) copolymers with varying molecular weight and chemical compositions (see Table 4)	
10	Ziegler–Natta based poly(ethylene- <i>co</i> -octene), multicatalyst poly(ethylene- <i>co</i> -octene), metallocene based poly(ethylene- <i>co</i> -octene) with 2.6 mol % octene	

materials in the low molecular weight regime (see Results and Discussion, Influence of Molecular Weight on Compositional Separation, for more details).

Comprehensive two-dimensional liquid chromatography has been used to provide two-dimensional maps of composition and molecular weight heterogeneity of copolymers,^{12–15} thus providing a more complete structural characterization of a polymer than a one-dimensional composition distribution and a one-dimensional molecular weight distribution. Because of this, such a two-dimensional map can provide structure–property insights that cannot be obtained from analysis of both of the one-dimensional distributions.

In the present work, one-dimensional HT–LC has been combined with high temperature gel permeation chromatography (HT–GPC) for the development of a comprehensive high temperature two-dimensional liquid chromatography (2D HT–LC) technique. The first dimension separation fractionates the polymer on the basis of chemical compositional heterogeneity while the second dimension separates comprehensive cuts of the first dimension by hydrodynamic size in solution. In contrast to other potential first dimension separation schemes based on crystallinity like CRYSTAF, TREF, or CEF, this gradient HTLC technique is readily applicable to both semicrystalline and amorphous polymers.

This report describes the method development and optimization aspects of the proposed system where the first dimension column is a Hypercarb column, and the second dimension column is a commercially available GPC column. Each fraction collected from the first dimension is transferred directly to the second dimension, providing a comprehensive cross-fractionation technique that can be realized in 8 h per sample. An off-line fractionation method based on fraction collection followed by conventional GPC could require hundreds of hours. Use of concentration and molecular mass-sensitive detectors (90° and 15° light scattering, linear IR absorbance) extend the quantitative ability to determine absolute weight-average molecular weight (M_w), weight fraction, and the radius of gyration of the eluted species. Although the light scattering detector can be used for absolute M_w , radius of gyration and solute conformation, these features were not exploited in this study. Use of molecular weight sensitive detectors in combination with 2D HT–LC may be the subject of future publications.

The 2D HT–LC approach borrows from previously reported 2D molecular topology fractionation (MTF) \times GPC.^{16,17} In 2D MTF \times GPC, separation was achieved in the first dimension based on long chain branching topological heterogeneity while the second dimension separation was based on hydrodynamic size and was applied to polyolefins at high temperature.¹⁶ Although there have been numerous reports involving comprehensive 2D LC, and in one example, the GPC dimension was performed at elevated temperature,¹⁸ the work reported here is the first to combine adsorption LC for composition fractionation

and GPC for size fractionation with both separation modes being performed at high temperature.

Co-crystallization is a phenomenon that can interfere with the determination of the composition distribution of semicrystalline polymers when separation techniques based on crystallization are used for characterization. When the cocrystallization artifact is operational, the less crystalline material can cocrystallize with the more crystalline material, and hence the composition distribution is distorted such that the apparent weight fraction of the higher crystallinity material is larger than expected. Separation of a pair of compositionally similar semicrystalline polyolefins (that can exhibit the cocrystallinity artifact in crystallinity based characterization schemes) in a manner free from the cocrystallinity artifact will be demonstrated.

Understanding the influence of catalyst type (e.g., Ziegler–Natta (ZN) versus metallocene) on the polymer molecular structure is another area of interest. Depending on the type of catalyst and the polymerization process, multimodal distributions in chemical composition and/or molecular weight can be produced. Complete resolution of these distributions is not always attainable by independent 1D analyses. Examples of the application of 2D HT LC to polyolefins made with different catalyst types will be presented here.

Experimental Section

Materials. 1-Decanol (>99% purity), ethylene glycol monobutyl ether (EGMBE) (>99% purity) and Ionol were purchased from Aldrich and used as received. HPLC grade 1,2,4-trichlorobenzene (TCB) was purchased from Fischer Scientific and recirculated through a 0.07- μ m nylon filter cartridge (Pall) before use. Table 1 provides a summary of the materials studied. Octene contents were determined using a previously described method.¹⁹ The weight-average molecular weight and polydispersity of the ethylene octene random copolymers used in optimization and calibration are provided in the Supporting Information (SI). Please see SI Table 1 for these data.

Sample Preparation. The samples were prepared in 1-decanol at a concentration of 3 mg/mL in 7 mL GPC vials. As they were prepared at room temperature, the volume expansion coefficient for 1-decanol was used to calculate the amount of 1-decanol required to reach the target concentration of 3 mg/mL at the autosampler temperature set point. Samples were then placed in a heated shaker for 2 h at 160 °C. Following the heating/shaking step, the vials were reheated on a heated plate equilibrated at 175 °C for 5–10 min. This step was useful in preventing the precipitation of the sample during handling and transferring of the vials from heated shaker to the heated injection carousel.

Equipment. Instrumentation. The instrumental setup for performing the 2D HT–LC–GPC experiments was developed through modifications to a Waters Alliance Model GPCV2000 (Milford, MA) HT–GPC system. The valve system for conducting the 2D HT–LC–GPC experiment is the same as that used for 2D MTF–GPC reported previously.¹⁶ The primary

Table 2. LC Gradient Programs Used in the Experiments

program 1-LC flow rate 0.02 mL/min			program 2-LC flow rate 0.015 mL/min		
time (min)	solvent A %	solvent B %	time (min)	solvent A %	solvent B %
0	100	0	0	100	0
200	0	100	266	0	100
225	0	100	299.25	0	100
226	100	0	300.25	100	0
258.5	100	0	343.8	100	0

Program 3-LC flow rate 0.01 mL/min			Program 4-LC flow rate 0.01 mL/min		
time (min)	solvent A %	solvent B %	time (min)	solvent A %	solvent B %
0	100	0	0	70	30
400	0	100	400	20	80
450	0	100	401	0	100
451	100	0	421	0	100
517	100	0	422	100	0
			488	100	0

injection of sample solution onto the first dimension column was accomplished with the internal injection valve of the HT-GPC. Two different injection volumes were tried: 20 and 100 μ L. The valve for injecting first dimension aliquots onto the second dimension column included a matched pair of 60- μ L injection loops which were alternately partially filled with 30 μ L of effluent from the first dimension column. Because of Poiseuille flow, 60- μ L loops were used to collect 30 μ L of effluent ensuring that the entire sample eluting from the first dimension column was injected onto the second dimension column. The effluent from the second dimension GPC column was continuously monitored by 15° and 90° laser light scattering (Precision Detectors, Model 2040, Bellingham, MA) and infrared absorbance (Polymer ChAR, Model IR4, Paterna, Spain) detectors. The IR4 detector was set to operate in concentration sensitive mode, where the measurement window included the C-H aliphatic bonds present in polyolefins but excluded the TCB solvent. The IR4 detector is a linear concentration detector that is an alternative to the refractive index detector for high temperature GPC of polyolefins.²⁰ The valves, columns, and detectors were all housed within the oven of the GPCV2000 instrument. A general description of the overall operational process has been reported elsewhere.¹⁶

LC Column. The graphitic carbon column discussed in this report was obtained from Thermo (Bethlehem, PA) and is described as a Hypercarb column with 250 Å pores, 5- μ m particles, and dimensions of 2.1 \times 100 mm.

GPC Column. The two GPC columns used in this study were purchased from Varian, Inc., Palo Alto, CA (Polymer Laboratories). Both columns were packed with PL-Gel mixed B resin. The first GPC column, used in experiments involving EGMBE as the weak solvent in the first dimension separation, was a PL MiniMix-B having dimensions (4.6 mm i.d. \times 250 mm length). The second GPC column, used in experiments involving 1-decanol as the weak solvent in the first dimension separation, was a PL Rapide H having dimensions of 10 mm i.d. \times 100 mm length.

PUMP. Two Shimadzu LC-20 AD pumps were used to provide the binary solvent (A: (EGMBE or 1-decanol) weak eluent and B (TCB): strong eluent) gradient for the first dimension. At least four different gradient programs were created and used for the experiments. Details are given in Table 2. The pump driving the GPC separation was the internal pump in the GPCV2000. TCB was used as eluent for the second dimension.

Data Acquisition and Reduction. Data acquisition for all of the detectors was performed using EZChrom Elite software from Agilent Technologies. Data files exported in ASCII format were processed in MATLAB (version 7.3) using custom written

routines for data folding and visualization of surface plots and contour maps. In addition to data folding and visualization, data files were baseline corrected, despiked (as necessary) and smoothed (as necessary) using custom written routines in MATLAB. Other custom-written MATLAB routines are discussed below.

The weak solvent used in the gradient solvent system was either EGMBE or 1-decanol. The samples were also prepared in 1-decanol. Both 1-decanol and EGMBE contain $-\text{CH}_2-$ groups which contribute a large solvent peak in the IR absorbance chromatogram. As a result, a MATLAB custom routine was written to remove the solvent peak from the GPC chromatograms. This was accomplished by specifying the "start" and "end" coordinates for the solvent peak position along the GPC axis. The removal of solvent peak enabled a much cleaner integration and plotting of the polymer signal without interference from the solvent peak. Following the solvent peak removal step, several other batch processing steps such as baseline correction, smoothing, and despiking were performed as needed.

Results and Discussion

Data Interpretation. The processed detector signals were folded and mapped using MATLAB (version 7.3) to generate the 3D surface map. A useful way to analyze the 2D data was from contour plots as shown in Figure 1 for IR absorbance data for a random ethylene octene copolymer with 14.8 mol % octene. Unlike NMR and other analytical tools which provide the average chemical composition, both quantitative chemical composition and molecular weight distribution, and the linkage between the two, are contained in the contour plots. In contrast, a 1D technique would have generated a single distribution curve that would not have allowed observation of the true two-dimensional relationships between composition and molecular weight. Additionally, a subroutine was written in MATLAB to mathematically sum the areas along the compositional and molecular weight axes to regenerate the one-dimensional composition-based and size-based chromatograms, respectively. The corresponding regenerated 1D chromatograms are also given in Figure 1.

Optimization Study. Experimental parameters were varied in order to obtain acceptable 2D separations. The experimental parameters studied were LC flow rate, GPC flow rate, valve-switching time, and GPC column type. The monitored responses included the separation of the polymer peak from the solvent peak stemming from the previous injection in the IR absorbance chromatograms and the baseline noise in the LS 90° scattering. The four sets of analyses with varying experimental parameters are given in Table 3.

For comprehensive 2D experiments, the hardware set up used during the study limited the injection volume for second dimension injections to 30 μ L. Although the injection loop size (for the second dimension) was 60 μ L, the loop was filled via Poiseuille flow,²¹ and therefore the linear flow speed down the center of the injection loop tube was twice the average linear flow speed. If radial mixing in the second dimension injection loop is not provided (no such provision was made), then one must expect Poiseuille flow to occur when the second dimension injection loop (a straight hollow tube) is filled with each new aliquot of first dimension effluent. If an attempt were made to load more than 30 μ L into the 60- μ L injection loop, then polymer material could be lost out the end of the injection loop, and therefore the 2D system would no longer be comprehensive. The dead volume of the second dimension injector loop does cause broadening in each GPC chromatogram generated in the second dimension, but the extent of

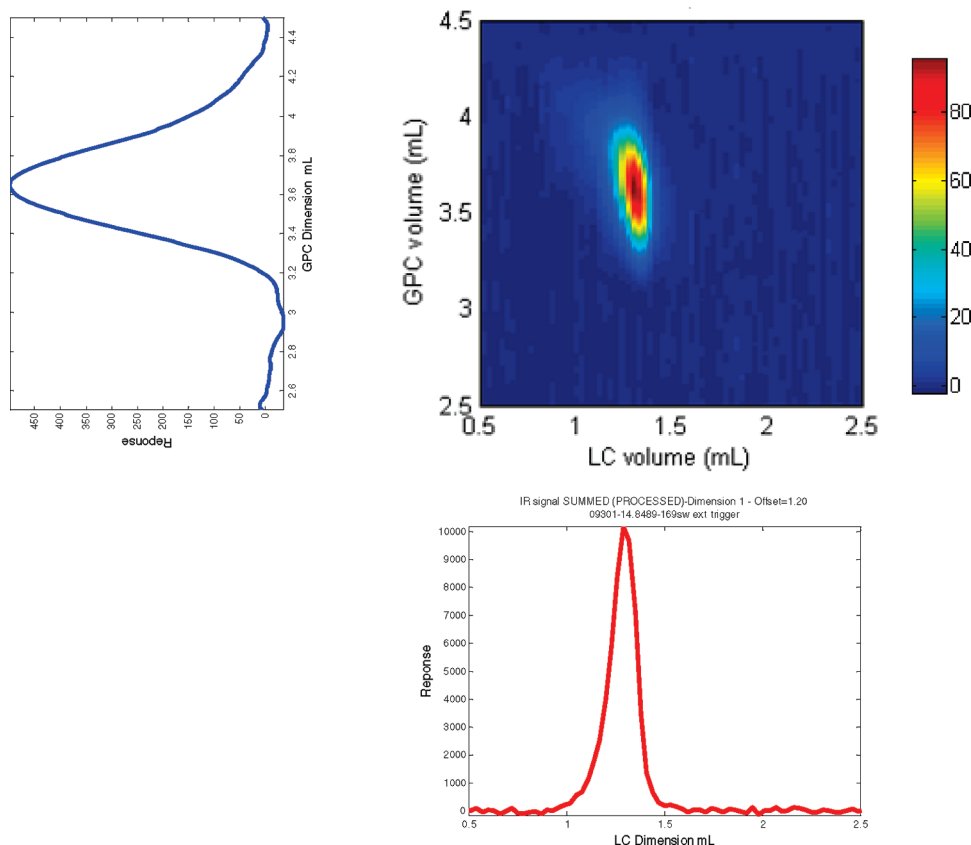


Figure 1. IR absorbance contour plot and corresponding 1D reconstructed chromatograms for both compositional (bottom) and molecular weight fractionation (upper left).

Table 3. Experimental Parameters Used for Optimization Experiments^a

no. of trial	LC flow rate (mL/min)	LC program	valve switching (min)	GPC flow rate (mL/min)	run time (min)
1	0.02	1	1.5	1.33	258.5
2	0.02	1	1.5	2.0	258.5
3	0.015	2	2	1.5	344
4	0.010	3	3	1.33	517

^a The LC programs (third column from left) can be found in Table 2.

broadening is not significant due to the fact that the total separation volume in the second dimension GPC column is much greater than the 60 μ L of the second dimension injector loop.

The second dimension injection volume which is a product of the LC flow rate and valve-switching time was kept constant for all four analyses. The experimental run time was dominated by the need to collect upward of 100 GPC chromatograms in the second dimension in order to maintain 100 or more resolution elements across the first dimension. The volume of eluent flowing through the GPC column between two successive second dimension injections is governed by the GPC flow rate and the valve-switching time. The temperature of the column was fixed at 140 °C, the carousel at 160 °C and the injector at 145 °C. The solvent used during sample preparation was 1-decanol and the EGMBE/TCB system was chosen as the gradient system.

The IR absorbance chromatograms for the four different experimental conditions, defined in Table 3, are provided in Figure 2. The solvent peaks were not removed by the software, but are deliberately shown such that the impact of experimental conditions on the elution of the polymer peak relative to the solvent peak from the previous injection can be

readily evaluated and observed. For run numbers 1 and 2, where the LC flow rate was higher than the latter two runs and the valve-switching time was kept at 1.5 min, the polymer peak was nearly engulfed within the solvent peak from the previous injection. The time between two successive injections was not long enough for the solvent peak to return to baseline before the polymer peak appeared from the next injection.

No improvement was observed by increasing the second dimension flow rate from 1.33 (run 1) to 2.0 mL/min (run 2). Significant improvement in polymer–solvent peak separation was observed as the valve switching time was increased to 2 and 3 min for runs 3 and 4, respectively. It is to be noted that for run 4, the volume of GPC eluent flowing between two successive injections was the highest at around 4 mL, based on the nominal GPC flow rate and valve-switching time. Maximizing the liquid volume flowing through the GPC column between successive injections enabled the solvent peak from the ($N - 1$)st injection to return to baseline prior to elution of the polymer peak from the N th injection. However, the GPC flow rate is ultimately limited by column pressure drop, the potential for shear degradation of the polymer and chromatographic broadening due to nonequilibrium between the flowing eluent and the stagnant eluent within the pores of the packing. To maintain adequate liquid volume between injections and integrity of the GPC separation, lower flow rates in the first dimension must be used.

The experimental results suggest that further improvement in polymer–solvent peak separation is possible by either increasing the valve-switching time or by increasing the volume of the liquid flowing through the GPC column between two successive injections. A further increase in valve-switching time (by > 3 min) would require either a

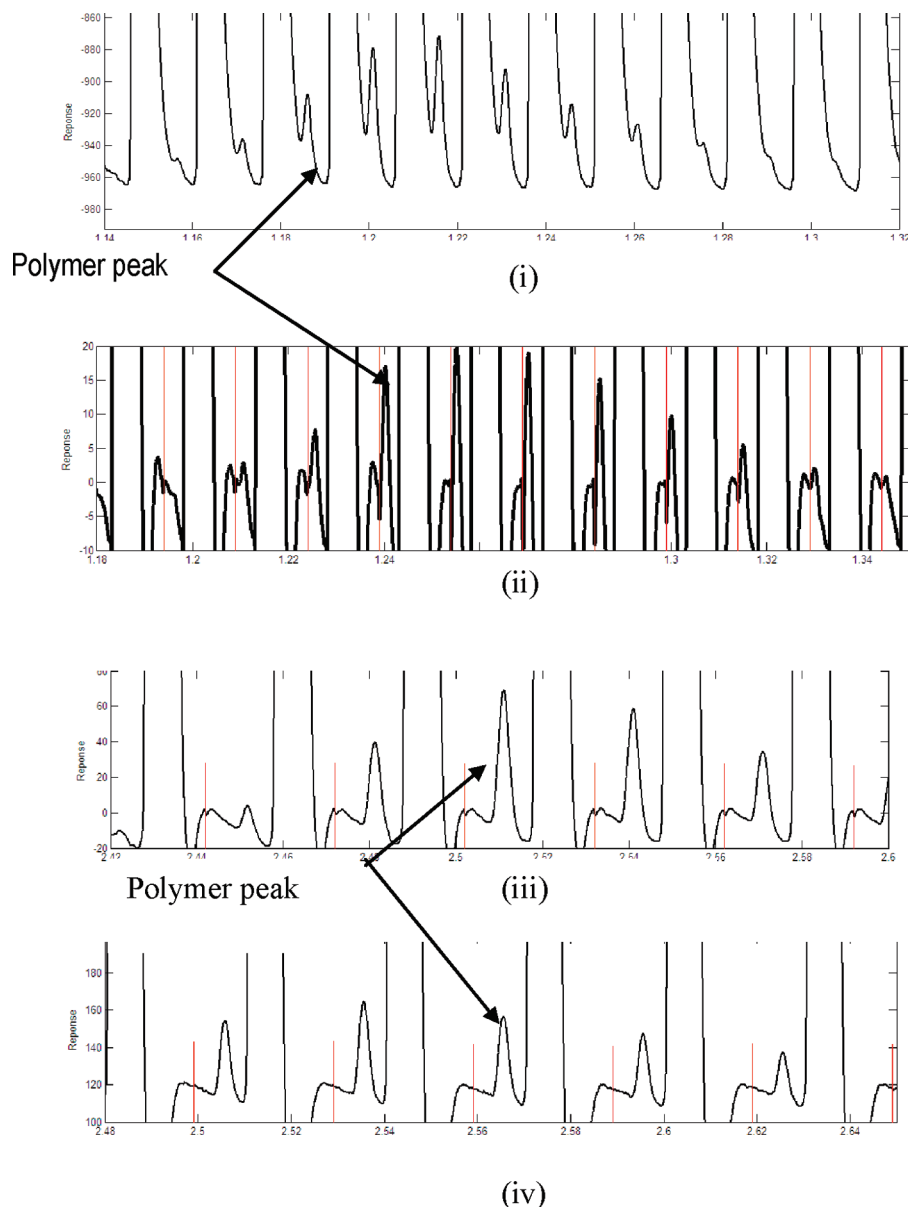


Figure 2. IR absorbance chromatograms for the optimization experiments. Conditions for trials i through iv are given in Table 3, experiments 1 through 4, respectively.

decrease in LC flow rate (to < 0.01 mL/min) or an increase of the second dimension loop volume. Increasing the second dimension injection volume was judged as unacceptable because of the resultant loss of resolution in both the first and second dimensions. Maintaining an accurate and reproducible first dimension solvent gradient was deemed important, and reducing the flow rate to below 0.01 mL/min could negatively affect the quality of the first dimension solvent gradient. Alternatively, the GPC flow rate could be increased to increase the volume of eluent flowing between two successive injections. The drawback of increased GPC flow rate would be a loss in second dimension resolution (as the linear velocity is increased), a subsequent increase in column pressure, and the potential to shear degrade polymer samples. However, this problem could be solved by increasing the GPC column diameter from 4.6 mm i.d. to 10 mm i.d. The larger column diameter would allow faster second dimension flow rates without changing the linear velocity, thus maintaining the separation capability. Although it is true that the larger i.d. column is shorter compared to the smaller i.d.

column, the reduction in plates due to the length decrease is more than offset by the increase in packing volume, and hence, pore volume. As a result, there is a net gain in GPC resolution,²² because GPC resolution is proportional to the reciprocal of the product $D\sigma$, where D is the slope of the calibration curve ($\log M$ versus retention volume for narrow standards) and σ is the standard deviation of a narrow standard. Enhanced GPC resolution is expected to improve the accuracy of determined molecular weight averages.

Although the initial runs were conducted at a temperature of 140 °C, specific applications may demand the use of higher temperature (e.g., 175 °C) and the 1-decanol/TCB gradient solvent system instead of EGMBe/TCB. No significant change in signal-to-noise ratio was observed for the LS response by going to a higher temperature. However, at the higher temperature, the IR signal for the polymer was engulfed in the solvent peak from the previous injection as shown in Figure 3A. The breadth of the solvent peak increased significantly resulting in overlap of the polymer peak with the solvent peak from the previous injection.

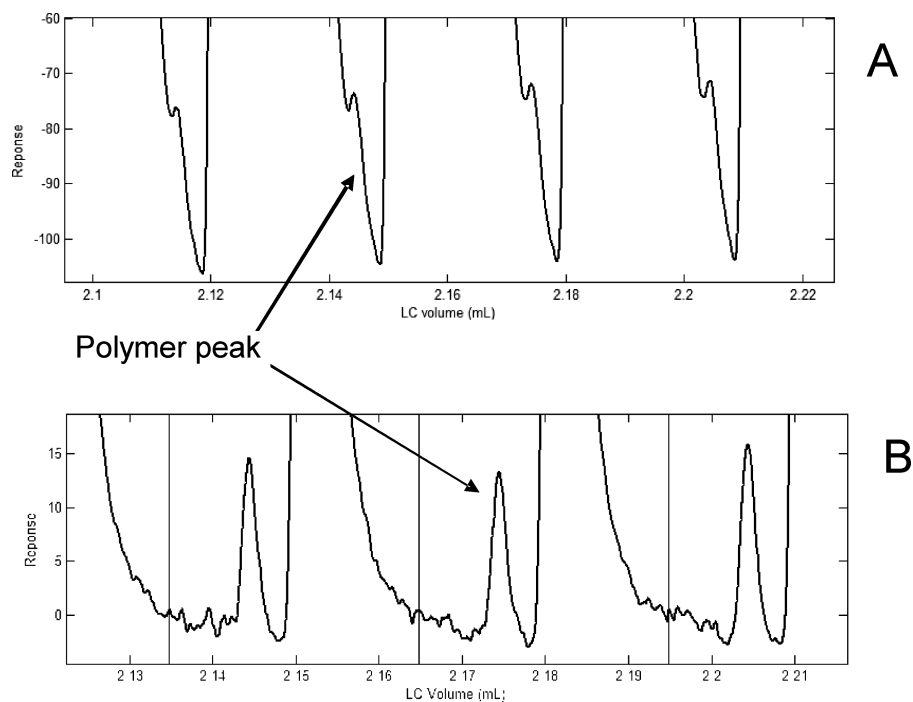


Figure 3. IR absorbance chromatograms for the same polymer sample run at 175 °C using a 4.6 mm i.d. \times 250 mm length GPC column (top A) and a 10 mm i.d. \times 100 mm length GPC column (bottom B). The LC flow rate was kept at 0.010 mL/min, GPC flow rate at 2.5 mL/min and valve switching time of 3 min.

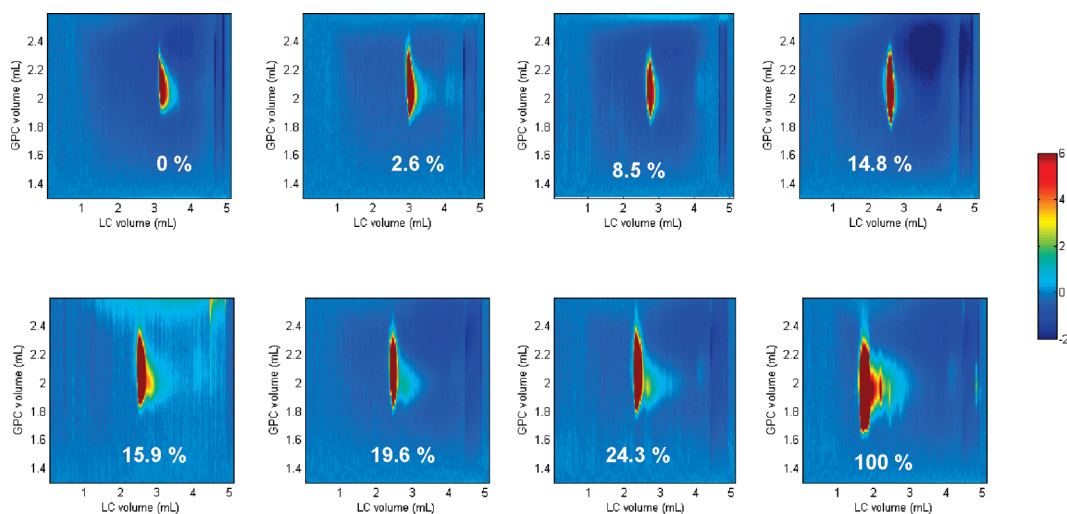


Figure 4. 2D 90° LS contour plots for a series of ethylene octene copolymers with varying octene mole percent.

Remarkable improvement in the separation between polymer and solvent peaks was observed by changing the column to the larger i.d. GPC column and by changing the GPC flow rate to 2.5 mL/min. As demonstrated in Figure 3B, the breadth of the solvent peak was much smaller and the higher flow rate achievable with this column allowed sufficient volume to flow through the column between successive injections enabling the polymer peak to elute in a region of relatively flat baseline.

2D HT LC–GPC Analysis for Ethylene Octene Random Copolymers. The main objective of this work was to demonstrate the capability of a 2D HTLC–GPC system to cross-fractionate polyolefins based on composition in the first dimension and based on molecular weight or size in the second dimension. A series of ten polyolefin samples, with varying octene content from 0 to 100%, was chosen for the study. The experimental parameters were kept identical to

the optimization trial 3 and the data were processed as discussed earlier. The temperature of the column was fixed at 140 °C, the carousel at 160 °C and the injector at 145 °C. The GPC column used was the MiniMix-B (see Experimental Section). The 2D contour plots of LS 90° scattering for EO random copolymers are given in Figure 4. Elution volume on the composition axis was a function of the octene content. The higher the octene content, the earlier the copolymer eluted on the LC axis. On the molecular weight axis, the copolymers eluted over a similar range of elution volume suggesting that they had similar molecular weights consistent with offline GPC analysis of the samples (See SI Table 1). For samples having octene contents up to and including 14.8%, unimodal distributions in chemical composition and molecular weight were observed. For samples having octene contents exceeding 14.8%, additional modes were observed in the contour plots. The additional modes

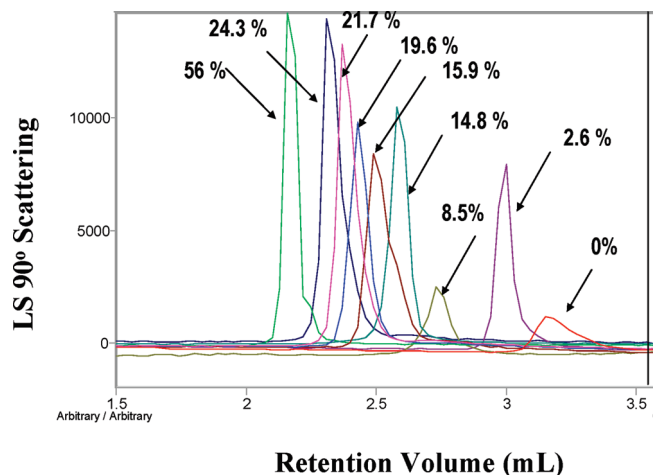


Figure 5. Reconstructed first dimension chromatograms from 90° LS data for EO copolymers with varying octene mole percent.

appeared to be lower in octene content and higher in molecular weight than the major component.

A 1D view of the resolution that was achieved in the first dimension of the 2D system can be observed in the overlay of mathematically regenerated 1D adsorption LC chromatograms given in Figure 5. As is evident, separation based on composition was achieved in the first dimension for both semicrystalline and amorphous copolymers. Near baseline separation was achieved between the homopolymer PE and EO copolymer with 2.6% octene content. These data reproduced the 1D work very well.⁹ In contrast, analytical temperature rising elution fractionation (ATREF) and CRYSTAF techniques resolve semicrystalline EO copolymers according to composition, but copolymers of ethylene containing more than about 8 mol % comonomer typically coelute as an unretained peak. The methodology in this report separates both amorphous and semicrystalline polyolefins according to composition.

A calibration curve was constructed from the peak apex retention times and their corresponding chemical composition values as determined by NMR. As demonstrated in Figure 6 the calibration curve was well described by a third order polynomial function from octene content 0–24.7%. This was an effective working range for most of the current polyolefins applications. This calibration added the capability to determine the chemical composition distribution of the whole sample or of any particular slice along the molecular size axis. The calibration could also be used to determine various compositional averages (either bulk or by size slice) using mathematics analogous to those used for determining molecular weight averages from GPC data.

The study was extended to construct 2D composition/molecular weight profiles at higher temperature (175 °C) using a short 1-decanol/TCB gradient in the first dimension (gradient program 4, Table 2) and using the 10 mm i.d. GPC column in the second dimension. The temperature of the column was fixed at 175 °C, the carousel at 175 °C and the injector at 175 °C. The LC flow rate was kept at 0.010 mL/min, GPC flow rate at 2.5 mL/min and valve-switching time of 3 min. The injection volume on the first dimension was 100 μ L. As discussed in Optimization, implementation of the higher pore volume, larger i.d. GPC column was essential to achieving polymer elution free of the solvent peak from the previous injection as observed in the IR absorbance response at this high temperature. The IR absorbance data for the EO copolymers over the octene composition range of

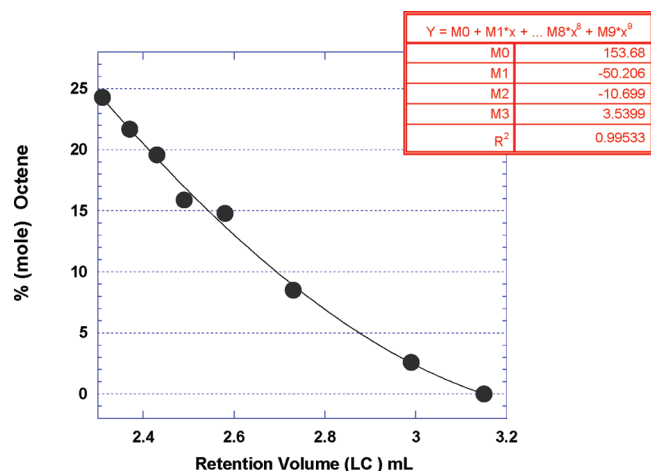


Figure 6. Calibration plot of octene content (NMR) vs first dimension peak retention volume.

2.6–19 mol % are given in Figure 7. For the low octene content materials, a curvature in the contour plots was observed. It appeared that a low molecular weight fraction was eluting slightly earlier than the higher molecular weight species. This low molecular weight fraction would not appear to be due to thermal degradation of the polymer, as repeat analyses of the same sample solution held in the 175 °C autosampler for 4X the amount of time as the original, yielded 2D contour plots that were indistinguishable from the original (data not shown). Additionally, for a given solution, total LS and IR peak volumes (total volumes under the surface plots) were independent of the amount of time the sample solution was held in the hot autosampler prior to injection. This finding suggests that the bulk M_w did not vary with time held at 175 °C.

Influence of Molecular Weight on Compositional Separation. To evaluate the effect of molecular weight on retention time in the first dimension, a series of metallocene catalyzed homopolyethylenes with varying molecular weights and polydispersities (M_w/M_n) near 2.0 were analyzed on the 2D HTLC–GPC system. Besides providing knowledge about molecular weight dependency on the compositional axis, the homopolyethylene samples enable calibration of the GPC axis for determining apparent molecular weight and distribution for the samples. The influence of molecular weight on compositional axis retention volume for the homopolyethylene samples is demonstrated in Figure 8a. A dependency was observed in the low molecular weight regime. However, for samples in the molecular weight range of 38 to 104 kg/mol, a negligible difference of 0.1 mL in retention volume was observed. As long as the molecular weight of the species is higher than approximately 40 kg/mol, orthogonality in the separation should be preserved, at least for homopolyethylene. A typical GPC type calibration plot of $\log(M_w)$ for the homopolyethylene standards versus the peak retention volume on the GPC axis is given in Figure 8b. As demonstrated, a linear calibration curve ($R^2 = 0.99$) was obtained. This curve could be used to determine apparent molecular weight distributions and molecular weight averages (either bulk, or for a given copolymer composition). The experimental parameters used included the following: gradient program 4 in Table 2; the temperature of the column was fixed at 175 °C, the carousel at 175 °C and the injector at 175 °C. The LC flow rate was kept at 0.010 mL/min, GPC flow rate at 2.5 mL/min (10 mm i.d. GPC column) and valve switching time of 3 min. The injection volume on the first injection was 100 μ L.

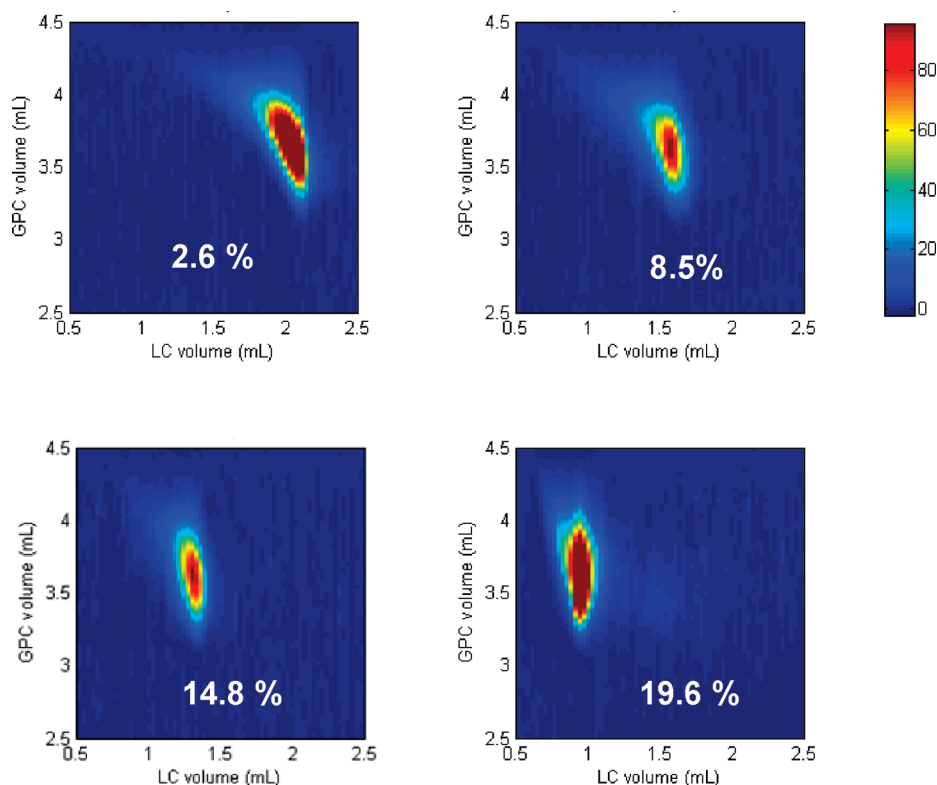


Figure 7. 2D contour plots of IR absorbance data for EO copolymers with varying octene content (the individual octene content is displayed in each plot).

Co-Crystallization. Co-crystallization is a phenomenon observed in crystallization-based techniques such as TREF, CEF and CRYSTAF that can interfere with the determination of the composition distribution of semicrystalline polymers. Polyolefin blends made from known amounts of semicrystalline narrow chemical composition materials that are similar in composition are often observed to cocrystallize during TREF, CEF, or CRYSTAF characterization experiments. For example, for a blend of known composition, the CRYSTAF determined apparent weight fraction of the more crystalline material will be higher than expected, suggesting a cocrystallization effect. In 2D HT–LC–GPC, the first dimension separation is hypothesized to be based on adsorption. As such cocrystallization would not be a contributing factor in elution. Furthermore, the separation is carried out at a temperature higher than T_M for all of the polymer materials present, and therefore it is impossible for crystals to be present. A 50:50 (weight basis) blend of materials that had demonstrated cocrystallization in CEF under certain conditions was prepared. The two samples differed in molecular weight and composition as given in Table 4.

The 2D contour plot for the blend sample is shown in Figure 9a. As seen, the two populations were well resolved on the compositional axis. No overlap was seen which suggested absence of the cocrystallization phenomena. The higher molecular weight species (sample A, Table 4) exhibited a narrow composition and broad molecular weight distribution. Curvature was seen in the contour plot for the lower molecular weight species (sample B, Table 4) indicating a slight molecular weight dependency on the compositional axis particularly at the low molecular weight regime. The 2D contour plot was used to reconstruct the compositional 1D chromatogram as illustrated in Figure 9b. Besides achieving baseline resolution, the quantified area under the curves for the two samples agreed to within 5%. Because a (50:50 wt %)

blend was used, the area under the individual resolved peaks should be equivalent in the absence of cocrystallization. As the experimental areas were equivalent to within 5%, it is reasonable to conclude that this technique demonstrates freedom from cocrystallinity for this pair of samples. The experimental parameters used included: gradient program 3, Table 2; the temperature of the column was fixed at 175 °C, the carousel at 175 °C and the injector at 175 °C. The LC flow rate was kept at 0.010 mL/min, GPC flow rate at 2.5 mL/min (10 mm i.d. GPC column) and valve switching time of 3 min. The injection volume on the first column was 100 μ L.

In this work, like virtually all chromatography work described in the literature, the retention mechanism cannot be stated with certainty. As a working hypothesis, the first dimension retention mechanism is believed to be adsorption. In support of this working hypothesis several reasons can be cited. First, the retention mechanism cannot be due to crystal formation as in CRYSTAF because the eluent temperature is always higher than T_M (the crystalline melting temperature of the polyolefins). Second, the retention mechanism cannot be due to precipitation followed by redissolution because the eluent composition provides solubility of the polyolefins at the operating column temperature long before the polymers ever elute from the first dimension. Third, others have formed a similar working hypothesis in the published literature.²³ Fourth, self-consistent-field simulations of the interaction of polyethylene chains (in the melt) with a graphite surface have shown a potential energy versus interaction distance plot that is strongly indicative of an adsorption interaction.²⁴ One might ask why poly(ethylene-co-octene) copolymers with low octene content are retained longer than ones with high octene content. Although the reason may not be stated with certainty, it is hypothesized that the presence of short chain branches along the polymer backbone provides steric hindrance to the process of orderly adsorption of

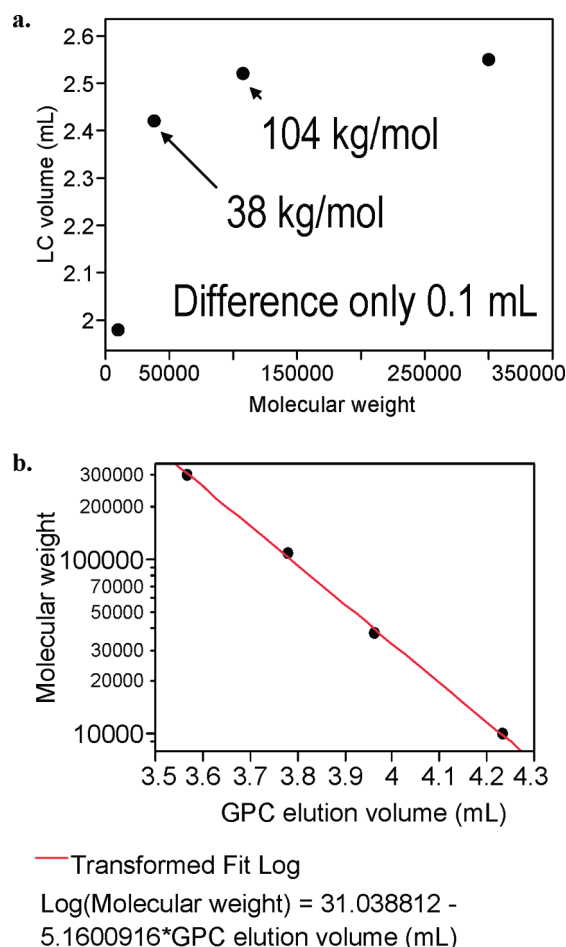


Figure 8. Influence of molecular weight on peak retention volume (a, top, compositional/1D axis; b, bottom, GPC axis).

Table 4. Characteristics of the Blend Sample Used to Demonstrate Freedom from Co-Crystallization

sample	M_w (kg/mol)	% C8
A	136	0.7
B	16.9	4.9

polyethylene chains on a graphite surface. The higher the mole fraction of side chains, the greater is the degree of steric hindrance, and therefore the weaker is the extent of adsorption interaction. Although the adsorption hypothesis described above was not proven with absolute certainty, it is consistent with the observations discussed here for composition based separations of polyolefins on a graphite column.

Other blends of materials that were known to cocrystallize during CEF characterization could not be resolved by adsorption LC. It appeared that crystallization techniques could perhaps provide slightly higher, apparent resolution than adsorption LC for polyolefins of low short chain branching content, but the crystallization based composition distributions were distorted due to the cocrystallization phenomenon, i.e., the higher crystallinity peak was too large and the lower crystallinity peak was too small. High resolution separation of a two component blend by adsorption liquid chromatography was difficult when the more crystalline component was relatively low in molecular weight ($< \sim 40$ kg/mol) while the less crystalline component was relatively high in molecular weight. Under this particular set of circumstances the lower molecular weight material eluted from the graphite column slightly earlier than expected for a

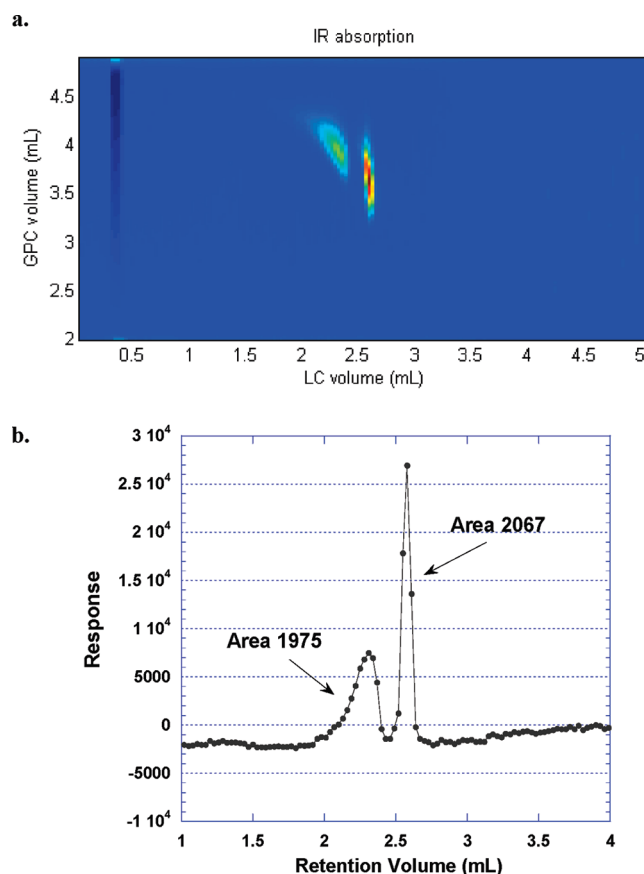


Figure 9. IR absorbance contour plots for a 50/50 weight% blend sample (top, a) and reconstructed 1D chromatogram for a 50/50 wt % blend sample (bottom, b) demonstrating freedom from cocrystallization.

high molecular weight, more crystalline material, and this caused coelution with the higher molecular weight and less crystalline component of the blend. Thus, the failure of the adsorption LC to provide resolution, in this particular case, was caused by the affect of molecular weight on first dimension retention time, but not by the cocrystallization phenomenon.

Influence of Catalyst Type on Molecular Structure. Polyolefins synthesized from different polymerization catalysts were also compared by this 2D HT LC–GPC technique. Three poly(ethylene-*co*-octene) samples were analyzed, including ZN based, multicatalyst based and metallocene based materials. All data shown in Figure 10 were generated using the LS 15° detector. For the ZN material, two to three resolved peaks were observed as shown in Figure 10a. It is hypothesized that these individual peaks are related to the different catalytic sites present in the ZN catalyst. When the multicatalyst sample was studied, three distinct peaks were observed (Figure 10b). Not only can the various composition modes in the 2D plot shown in Figure 10b be observed, but one can also observe the relative molecular weight distributions for each of the composition modes. In contrast, a one-dimensional molecular weight distribution of the multicatalyst sample would result in a single-mode broad peak from which one could not decipher the molecular weight profiles of the individual compositional modes. For the single site metallocene catalyst sample (Figure 10c) only one peak was observed. The experimental parameters used included the following: gradient program 4, Table 2; the temperature of the column was fixed at 175 °C, the carousel at 175 °C and the injector at 175 °C. The LC flow rate was kept at

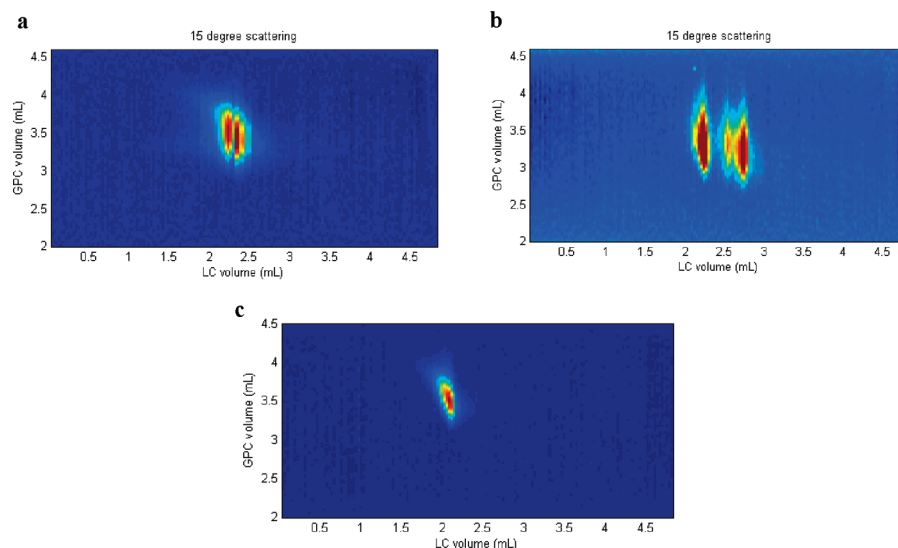


Figure 10. 2D contour plots (15° LS) for polyolefins synthesized from different types of catalysts: (a) Ziegler–Natta based poly(ethylene-*co*-octene), (b) multicatalyst based poly(ethylene-*co*-octene), and (c) metallocene based poly(ethylene-*co*-octene) with 2.6 mol % octene.

0.010 mL/min, GPC flow rate at 2.5 mL/min (10 mm i.d. GPC column) and valve-switching time of 3 min. The injection volume on the first column was 100 μ L.

Conclusions

This paper is a continuation and extension of the high temperature liquid gradient chromatography work developed for polyolefin separation, particularly for copolymers with high octene content. Complementing the one-dimensional work, which separated polyolefins based on their differences in composition, a two-dimensional high temperature liquid chromatography method was developed. Separation was achieved based on composition in the first dimension and on molecular size in the second dimension. The instrumentation and software development was adapted from the existing 2D MTF \times GPC technology. Several custom MATLAB routines were written specifically for this current 2D HTLC technique. The LC or the first-dimensional axis was calibrated with EO standards with known composition (from NMR). Similarly the GPC axis was calibrated with PE standards with varying molecular weights.

A series of PE random copolymers with varying ethylene octene content was studied. Separation based on octene content in the first dimension and on molecular weight in the second dimension was achieved. 2D contour plots were constructed for samples which provided knowledge of both apparent chemical composition and molecular weight at the same time. Software was developed to regenerate one-dimensional chromatograms for both chemical composition and molecular weight. The regenerated 1D chromatograms provide simplified views of the two-dimensional data and allowed for peak area integration.

The technique demonstrated a significant potential for elimination of the effect of cocrystallization on a composition based separation. Indeed, above T_M there can be no cocrystallization because the polymers cannot exist as crystals above T_M . Baseline separation with a proper peak area ratio was achieved for a pair of EO copolymers demonstrating the absence of cocrystallinity. That particular pair exhibited cocrystallization with CEF under certain conditions.

This 2D HTLC–GPC technique was also utilized to study the structural differences between poly(ethylene-*co*-octene) materials synthesized from different types of catalysts. Polyolefins synthesized from ZN, multicatalyst systems, and metallocene showed differences in the number of resolved

populations, and in the molecular weight and composition profiles of the populations.

Acknowledgment. The authors thank the management of The Dow Chemical Company for funding this work.

Supporting Information Available: A table giving additional information about the characterization of the ethylene octene random copolymers. This material is available free of charge via the Internet at <http://pubs.acs.org>.

References and Notes

- Lyons, J. W.; Poche, D.; Wang, F. C. Y.; Smith, P. B. *Adv. Mater. (Weinheim, Ger.)* **2000**, *12*, 1847–1854.
- Gillespie, D. T.; Li Pi Shan, C.; Hazlitt, L. G.; DeGroot, A. W.; Arnoudse, P. B.; Williams, C. A. PCT Patent Application: Apparatus for method for polymer characterization. WO 2006/081116 A1.
- Monrabal, B.; Sancho-Tello, J.; Mayo, N.; Romero, L. *Macromol. Symp.*, **2007**, *257* (Polyolefin Characterization), 71–79.
- Cong, R.; DeGroot, A. W.; Klinker, C. M.; Yau, W.; Hazlitt, L.; Lyons, J. W.; Monrabal, B. *Abstracts of Papers, 236th ACS National Meeting, Philadelphia, PA, United States, August 17–21, 2008*; American Chemical Society: Washington, DC, 2008; ANYL-248.
- Hazlitt, L. G. *J. Appl. Polym. Sci.: Appl. Polym. Symp.*, **1990**, *45* (Polym. Anal. Charact. 2), 25–37.
- Monrabal, B. *J. Appl. Polym. Sci.* **1994**, *52*, 491–499.
- Monrabal, B. *Macromol. Symp.*, **1996**, *110* (10th Bratislava International Conference on Macromolecules: Chromatography of Polymers and Related Substances, 1995), 81–86.
- Miller, M. D.; DeGroot, A. W.; Lyons, J. W.; van Damme, F.; Winniford, B.; Pasch, H.; Macko, T. *Abstracts of Papers, 236th ACS National Meeting, Philadelphia, PA, United States, August 17–21, 2008*; American Chemical Society: Washington, DC, 2008; ANYL-246.
- Miller, M. D.; Lyons, J. W.; DeGroot, A. W.; Winniford, W. L.; Herceg, E. Separation of polyolefins based on comonomer content using high-temperature gradient adsorption liquid chromatography with a graphitic carbon column. *J. Appl. Polym. Sci.* Manuscript in preparation.
- Pasch, H.; Albrecht, A.; Bruell, R.; Macko, T.; Hiller, W. *Macromol. Symp. Macromol. Symp.* **2009**, *282*, 71–80.
- Macko, T.; Brüll, R.; Alamo, R. G.; Thomann, Y.; Grumel, V. *Polymer* **2009**, *50*, 5443–5448.
- Kok, S. J.; Hankemeier, Th.; Schoenmakers, P. J. *J. Chromatogr., A* **2005**, *1098* (1–2), 104–110.

- (13) Jiang, X.; Van der Horst, A.; Lima, V.; Schoenmakers, P. J. *J. Chromatogr., A* **2005**, *1076* (1–2), 51–61.
- (14) Raust, J.-A.; Bruell, A.; Moire, C.; Farcet, C.; Pasch, H. *J. Chromatogr. A* **2008**, *1203* (2), 207–216.
- (15) Gao, H.; Louche, G.; Sumerlin, B. S.; Jahed, N.; Golas, P.; Matyjaszewski, K. *Macromolecules* **2005**, *38*, 8979–8982.
- (16) Meunier, D. M.; Stokich, T. M., Jr.; Edam, R.; Schoenmakers, P. J.; Gillespie, D.; deGroor, W. *Polym. Prepr. (Am. Chem. Soc., Div. Polym. Chem.)* **2008**, *49*, 131–132.
- (17) Edam, R.; Meunier, D. M.; Mes, E. P. C.; van Damme, F. A.; Schoenmakers, P. J. *J. Chromatogr., A* **2008**, *1201*, 208–214.
- (18) Im, K.; Park, H.-W.; Lee, S.; Chang, T. *J. Chromatogr. A* **2009**, *1216*, 4606–4610.
- (19) Qiu, X. H.; Zhou, Z.; Gobbi, G.; Redwine, O. D. *Anal. Chem.* **2009**, *81*, 8585–8589.
- (20) Yau, W. W. *Macromol. Symp.* **2007**, *257*, 29–45.
- (21) Perry, R.; Green, D. *Perry's Chemical Engineer's Handbook*, 6th ed.; McGraw-Hill: New York, 1984, p 23, equation 5–53.
- (22) Yau, W. W.; Kirkland, J. J.; Bly, D. D. *Modern Size-Exclusion Liquid Chromatography Practice of Gel Permeation and Gel Filtration Chromatography*; Wiley: New York, 1979. See Chapter 4, Resolution.
- (23) Macko, T.; Pasch, H. *Macromolecules* **2009**, *42*, 6063–6067.
- (24) Daoulas, K. Ch.; Theodorou, D. N.; Harmandaris, V. A.; Karayiannis, N. Ch.; Mavrantzas, V. G. *Macromolecules* **2005**, *38*, 7134–7149.